# European high-impact weather caused by the downstream response to the extratropical transition of North Atlantic Hurricane Katia (2011)

Christian M. Grams[1] and Sandro R. Blumer[1,2,3]

[1]Institute for Atmospheric and Climate Science, ETH Zurich, Zurich, Switzerland, [2]Climate and Environmental Physics, University of Bern, Bern, Switzerland, [3]Oeschger Centre for Climate Change Research, Bern, Switzerland

**Abstract** Tropical cyclones undergoing extratropical transition (ET) are thought to cause high-impact weather (HIW) close to the transitioning tropical cyclone and in remote regions. However, no study so far clearly attributed European HIW to the *downstream* impact of North Atlantic ET. When Hurricane Katia underwent ET in September 2011, severe thunderstorms occurred downstream in Central Europe. We quantify the role of Katia in the European HIW, using numerical sensitivity experiments. Results show that Katia was crucial for the evolution of a narrow downstream trough. Large-scale forcing for ascent ahead of this trough triggered deep convection. In the absence of ET, no trough was present over Europe and no HIW occurred. This study is the first unambiguous documentation that European HIW is *caused* by the *downstream* impact of North Atlantic ET and would not occur otherwise. It likewise corroborates the crucial role of ET in altering the large-scale midlatitude flow in downstream regions.

## 1. Introduction

In the North Atlantic about 46% (4–5 per year [*Hart and Evans*, 2001]) of all tropical cyclones (TCs) transform into an extratropical cyclone, a process that is referred to as extratropical transition (ET) [*Jones et al.*, 2003]. During ET, a TC gradually looses its symmetric, warm-core tropical characteristics and becomes an asymmetric, baroclinic extratropical cyclone [e.g., *Klein et al.*, 2000; *Evans and Hart*, 2003].

Predictability for the midlatitude flow is often reduced during ET [*Anwender et al.*, 2008; *Keller et al.*, 2011; *Aiyyer*, 2015; *Grams et al.*, 2015]. This is due to model sensitivity to the interaction of the transitioning TC with the upper-level midlatitude flow. In the potential vorticity (PV) perspective, this interaction is manifested in diabatic PV modification due to the strong latent heat release in the transforming TC's inner core. At upper levels PV is diabatically reduced and the low-PV air is advected poleward by the TC outflow [*Atallah and Bosart*, 2003; *Agustí-Panareda et al.*, 2004]. This process results in the formation of an upper-level ridge directly downstream of the transforming TC. Likewise, an upper-level midlatitude jet streak evolves and the upstream trough amplifies, often resulting in a favorable environment for extratropical reintensification. In an Eulerian-Lagrangian PV perspective *Grams et al.* [2013a, 2013b] stressed that vertical upright ascent in the TC inner core is gradually replaced by slantwise ascent along the midlatitude baroclinic zone during and after ET, maintaining the diabatic outflow aloft that is key to the net transport of low-PV air to the tropopause, associated ridgebuilding, and jet acceleration.

In the presence of a strong TC-extratropical flow interaction, the ridgebuilding triggers downstream development of a pronounced Rossby wave train [*Archambault et al.*, 2013, 2015; *Quinting and Jones*, 2015; *Torn and Hakim*, 2015]. Differences exist for different ocean basins. For example, *Quinting and Jones* [2015] showed that a statistically significant increase and amplification of Rossby wave packets exist in the North Pacific and South Indian Ocean but not in the North Atlantic. The downstream impact of ET is governed by Rossby wave dynamics [*Thorncroft et al.*, 1993] and explored in detail by various authors [e.g., *Riemer et al.*, 2008; *Riemer and Jones*, 2010; *Harr and Dea*, 2009; *Keller et al.*, 2014; *Archambault et al.*, 2015; *Torn and Hakim*, 2015]. It also critically depends upon the phasing of the recurving TC and midlatitude flow features [e.g., *Klein et al.*, 2002; *Ritchie and Elsberry*, 2007; *Grams et al.*, 2013a; *Archambault et al.*, 2015].

Many case studies documented high-impact weather (HIW, e.g., heavy precipitation) directly related with North Atlantic ET, i.e., in Northeastern America [*DiMego and Bosart*, 1982; *Bosart and Lackmann*, 1995;

*McTaggart-Cowan et al.*, 2001; *Atallah and Bosart*, 2003; *McTaggart-Cowan et al.*, 2004] or in Europe [*Browning et al.*, 1998; *Thorncroft and Jones*, 2000; *Agustí-Panareda et al.*, 2005].

However, only few studies exist that clearly document the role of ET in triggering HIW in regions downstream and remote of the actual transitioning TC. In the non-peer-reviewed literature, *Archambault* [2007, 2011], *Grams* [2011], or *Keller and Grams* [2014] documented different western North Pacific ET cases that each triggered a highly amplified ridge over western North America and were associated with a cold air outbreak at the eastern flank of this ridge. *Cordeira and Bosart* [2010] showed that a highly amplified Rossby wave train, triggered by a series of western North Pacific ETs, was crucial for the formation of the "Perfect Storms" at the U.S. East Coast in November 1991. For the Atlantic-European region, *Hoskins and Berrisford* [1988] indicated that the ET of Hurricane Floyd (1987) was important in the downstream development of an extratropical cyclone devastating southern UK in October 1987. *Agustí-Panareda et al.* [2004] mentioned that a downstream cyclone was more intense in the presence of the ET of Hurricane Irene (1999). *Stohl et al.* [2008] highlighted the crucial role of North Atlantic ET events in forming a so-called atmospheric river that led to heavy precipitation at the Norwegian coast. *Grams et al.* [2011] documented the role of Hurricane Hanna in amplifying a PV streamer that eventually triggered a Mediterranean cyclone. However, the ET rather shifted the location of regions affected by HIW than causing it. A similar result was found by *Pantillon et al.* [2015] who assessed the role of several North Atlantic ET in triggering Mediterranean cyclogenesis during 2012 and concluded that North Atlantic ET is rather a perturbation to Mediterranean cyclogenesis than its cause. To the knowledge of the authors no study so far was able to clearly attribute a European HIW event to the *downstream* impact of North Atlantic ET, i.e., answered the question "Can European HIW be caused by the downstream impact of North Atlantic ET?"

In the manuscript at hand, we answer this question for Hurricane Katia in September 2011. The data and diagnostics are briefly explained in section 2. In section 3 we give an overview of the ET of Hurricane Katia and document European HIW in the same period. The role of Katia in European HIW is quantified in section 4. We then explore the physical processes that are responsible for the HIW (section 5) and end with a brief discussion and our main conclusions (section 6).

## 2. Data and Methods

This study uses operational European Centre for Medium-Range Weather Forecast (ECMWF) high-resolution analysis data, interpolated on a 0.25° × 0.25° latitude-longitude grid. The ECMWF analysis provides initial and boundary conditions for simulations with the limited area model COSMO (Version 4.18) [*Steppeler et al.*, 2003]. In addition, NOAA Climate Data Record (CDR) of Gridded Satellite Data from ISCCP B1 (GridSat-B1) 11 micron Brightness Temperature, Version 2 are used [*Knapp et al.*, 2011].

Two COSMO simulations are performed, a control simulation (CTRL) and a simulation with Hurricane Katia removed from the initial conditions (NOTC), using the TC removal method of *Grams et al.* [2013b]. Details on the setup of the TC removal are given in Text S1 in the supporting information. As in previous studies [e.g., *Wu and Kurihara*, 1996; *McTaggart-Cowan et al.*, 2001; *Klein et al.*, 2002; *Agustí-Panareda et al.*, 2004; *Grams et al.*, 2011, 2013b; *Pantillon et al.*, 2015], we attribute the differences between the two simulations to the impact of ET on the midlatitude flow. The simulations are initialized at 00 UTC, 8 September 2011, well before strong TC-midlatitude flow interaction occurred (cf. Text S3 and Table S1 of *Grams et al.* [2015]). The model domain extends over North America, the North Atlantic, and Europe (−138°E to 48°E, 10°N to 75°N) at 0.25° horizontal grid spacing (745 × 261 grid points) and 80 vertical levels.

As in *Böttcher and Wernli* [2011] and *Grams et al.* [2013a], a diagnostic based on the height-attributable solution [*Clough et al.*, 1996] of the quasi-geostrophic (QG) omega equation in Q-vector form [*Hoskins et al.*, 1978] is used to estimate upper-level forcing for ascending motion. The contribution to vertical velocity from the upper troposphere ($\leq 650$ hPa) is evaluated at 700 hPa following *Deveson et al.* [2002] and *Dacre and Gray* [2009].

## 3. The Extratropical Transition of Hurricane Katia
### 3.1. Overview
An overview of Katia's life cycle is given based on information from the National Hurricane Center tropical cyclone report by *Stewart* [2012].

Hurricane Katia was a long-lived Cape Verde Hurricane that remained over the open Atlantic Ocean for its entire tropical lifetime (Figure S1a in the supporting information). Katia formed on 28 August 2011 off the
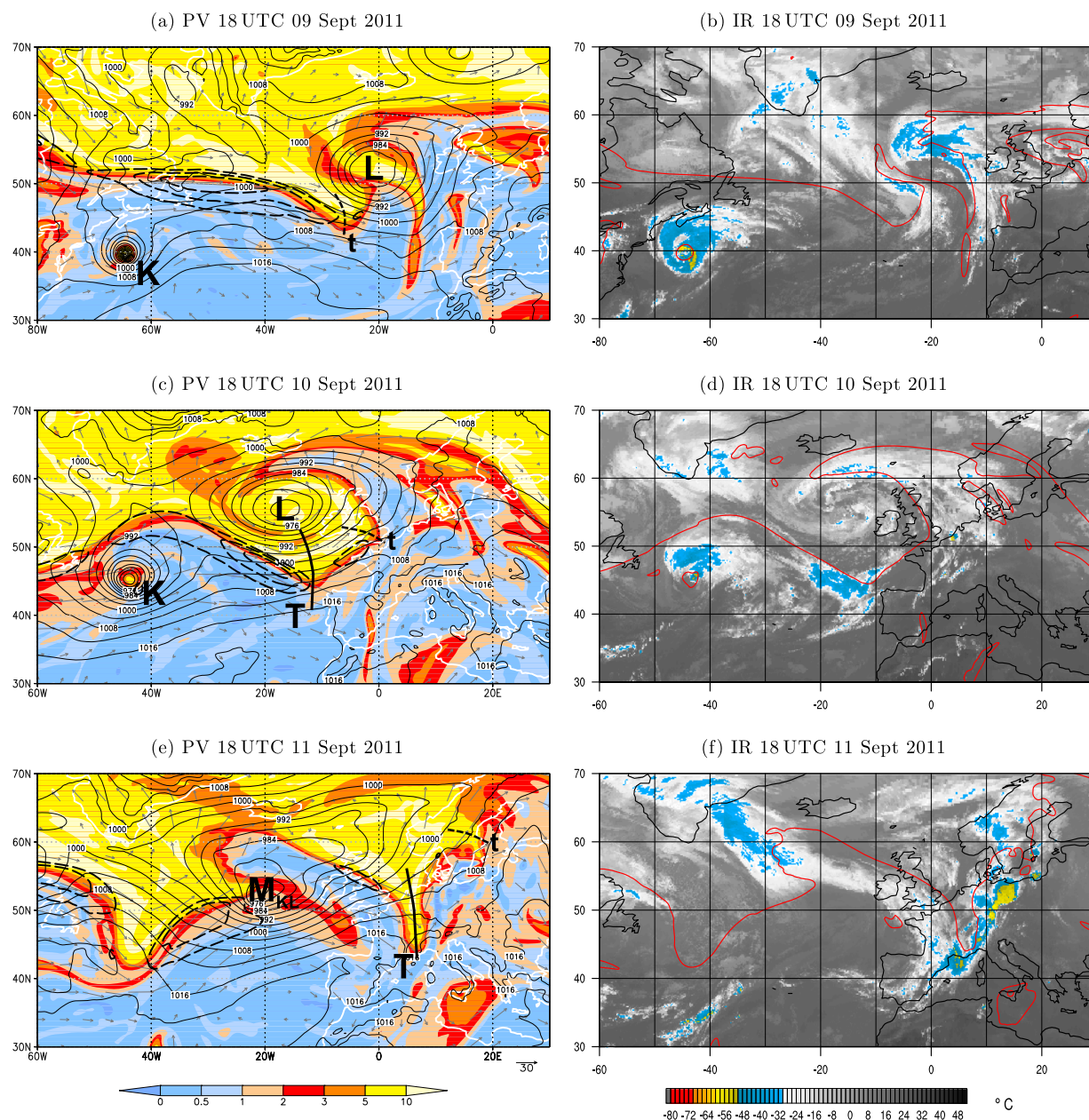
**Figure 1.** (left) PV (in PVU, shaded), wind (grey vectors and black dashed with a 10 m s$^{-1}$ contour interval starting at 50 m s$^{-1}$) at the 335 K isentropic surface, and pmsl (black contours every 4 hPa) in ECMWF analysis. (right) IR satellite imagery based on Gridsat B1 data, 3 PVU contour (red) on the 335 K isentropic surface (ECMWF analysis). (a) 18 UTC, 9 September 2011, (b) 18 UTC, 10 September 2011, and (c) 18 UTC, 11 September 2011. Label "K" marks Hurricane Katia, "L" cyclone Frank, "M$_{KL}$" the merger cyclone, "T"/"t" and the black axis the downstream/short-wave trough, respectively. Note the shift in the domain displayed in Figures 1a, 1b; 1c, 1d; and 1e, 1f.

Coast of West Africa from a tropical wave and headed westward under steady intensification. On 1 September 2011 Katia was declared a Hurricane and started to track northwestward. On 6 September Katia reached peak intensity with an estimated center pressure of 942 hPa. Two days later, Katia recurved at around 70°W, 33°N onto a northeastward track and was declared extratropical at 12 UTC on 10 September 2011. During the transition into an intense extratropical cyclone Katia reintensified. Its center pressure dropped from 969 hPa (18 UTC, 7 September) to 954 hPa (12 UTC, 10 September). Katia finally passed close to the northern British Isles on 12 September 2011 and merged with a mature extratropical cyclone ("Frank") between Iceland and the British Isles.

### 3.2. Extratropical Transition

The period of Katia's ET is discussed with a 24-hourly sequence of PV and wind on the 335 K isentropic surface, pressure at mean sea level (pmsl), and IR satellite imagery (Figure 1). Dense contours of PV, centered around 2 to 5 PVU in Figures 1a, 1c, and 1e (red shades), mark the intersection with the dynamical tropopause and the midlatitude waveguide. South of the waveguide, the 335 K isentropic surface is located at about 400 hPa in the subtropical upper troposphere, it rises to about 250 hPa in the extratropical lower stratosphere to the north.

At 18 UTC, 9 September 2011, Katia is located at about 65°W, 40°N with a center pressure of 960 hPa (labeled "K," Figure 1a). To the north the midlatitude upper-level flow is almost zonally aligned with a marked jet streak along 51°N. Katia still exhibits tropical characteristics as reflected in the symmetric shape of 335 K PV, pmsl, and high clouds (Figures 1a and 1b). However, Katia's upper-level outflow becomes directed northeastward (wind vectors in Figure 1a) and a cirrus cloud shield (Figure 1b) expands toward the jet streak to the northeast. Farther downstream, extratropical cyclone Frank (labeled "L", Figure 1a) and a short-wave trough (labeled "t") are the most prominent weather systems in the East Atlantic.

One day later, Katia is located ahead of an upper-level trough and transformed into an intense extratropical cyclone ("K", 44°W, 45°N, 954 hPa; Figure 1c). To its northeast, diabatic outflow results in upper-level ridgebuilding and maintenance of the western part of the jet streak directly downstream of the transitioning TC, as reflected in low-PV air and a westward extension of the 50 m s$^{-1}$ isoline (Figure 1c). Farther to the east, a downstream trough (labeled "T", Figure 1c) amplifies while the short-wave trough propagates eastward (labeled "t"). Frank became a mature extratropical cyclone west of the British Isles. Katia lost its tropical characteristics (Figure 1d). An asymmetric cloud shield expands over the region of the ridge directly downstream of Katia, reflecting diabatic outflow of ascending air in the evolving warm sector. To the West of Katia partly cloud-free regions indicate the equatorward advection of cool, dry polar air. A line of higher clouds to the southwest of Katia marks the formation of a weak cold front.

Until 18 UTC, 11 September 2011, Katia merged into extratropical cyclone Frank and weakened (21°W, 53°N, 966 hPa; labeled "$M_{KL}$," Figure 1e). The ongoing ridgebuilding to the northeast of Katia results in an important amplification of the downstream trough "T" that became a narrow PV streamer over Europe with its axis along 5°E (Figure 1e). Low-PV air to the east of this PV streamer indicates diabatic outflow due to deep convection ahead of the PV streamer. The deep convection is reflected in very low IR brightness temperatures over eastern Germany and western Poland (Figure 1f). The short-wave trough ("t") is now located over the Baltic Sea.

### 3.3. High-Impact Weather

Katia had no reported impact on human activities as a tropical cyclone. However, Katia had severe *direct* impact over the northern British Isles during extratropical stage [*Stewart*, 2012].

Severe high-impact weather also occurred farther *downstream* but has not been associated with the ET of Katia yet. On 11 September 2011 intense thunderstorms formed in Central Europe ahead of the narrow upper-level trough ("T", Figures 1e and 1f) causing property damage, rail and road closures due to mudslides, and local flooding [*Ehmann and Mühr*, 2011]. The most severe convection occurred in Central and Eastern Germany where 1-hourly rainfall of more than 30 mm and 24 h rainfall of more than 45 mm were observed ([*Ehmann and Mühr*, 2011], and cf. Figure 3a). Hail with diameter of 5 – 8 cm was reported, wind gusts exceeded 30 m s$^{-1}$, and very high frequencies of lightning occurred along with the deep convection in Eastern Germany [*Ehmann and Mühr*, 2011]. Moreover, at least one confirmed tornado formed in this region. In the remainder we will show that the HIW in Central Europe was caused by an important *downstream* impact of the ET of Katia.

## 4. Quantification of Katia's Impact on the Midlatitude Flow

In this section we employ the TC removal technique (section 2 and Text S1 in the supporting information) to quantify the role of Katia's ET in the formation of the narrow downstream upper-level trough and associated severe convection in Central Europe. We investigate differences in PV and wind on the 335 K isentropic surface between the CTRL simulation with ET and the NOTC simulation without ET. The CTRL simulation accurately represents the actual ET during the period of interest as verified against ECMWF analysis, based on TC track and the large-scale flow pattern (cf. supporting information Text S2, Figures S1, S2, and *Blumer* [2013] and *Grams et al.* [2015]).
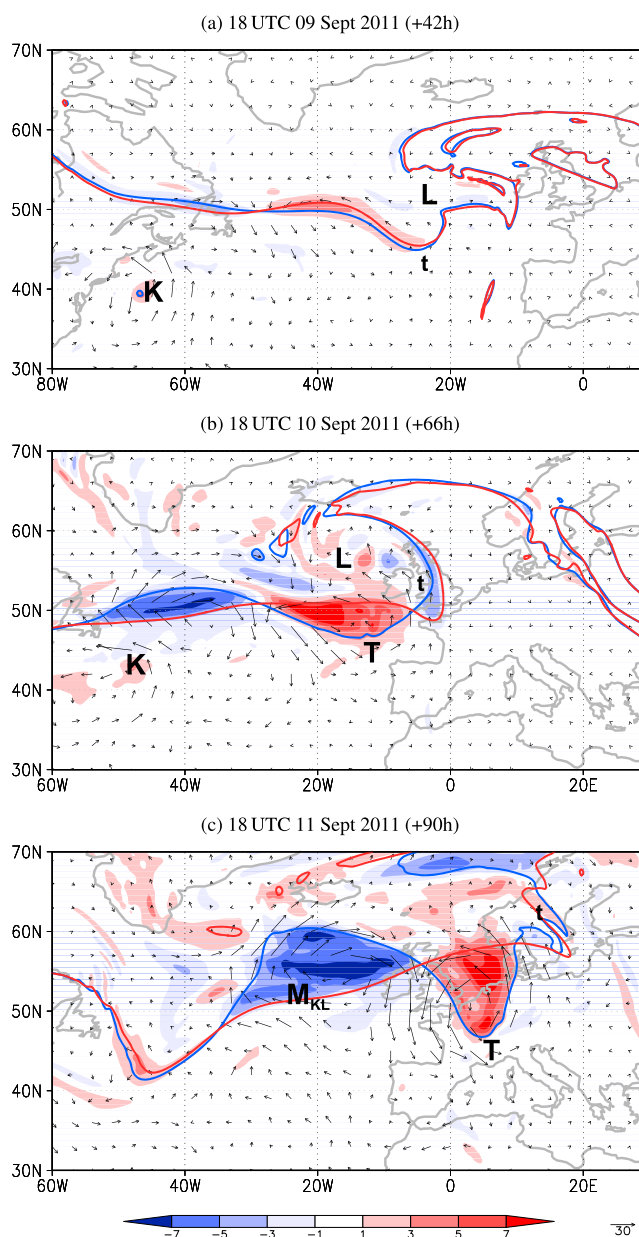
**Figure 2.** Difference (CTRL minus NOTC simulation) of PV (shaded, in PVU) and difference wind vectors (black) at the 335 K isentropic surface. The 4 PVU contour on 335 K of the CTRL simulation is shown in blue and of the NOTC simulation in red. (a) 18 UTC, 9 September 2011, (b) 18 UTC, 10 September 2011, and (c) 18 UTC, 11 September 2011. Location of main weather systems in CTRL marked with labels as in Figure 1.

At the early stage of ET (18 UTC, 9 September 2011, Figure 2a), little differences exist for the upper-level mid-latitude flow between CTRL and NOTC. As in the analysis, both simulations exhibit strong zonal flow to the north and northeast of Katia and a weak short-wave trough farther downstream (labeled "t," axis at 25°W, Figure 2a, cf. Figures 1a and 1b). However, negative difference PV (blue shading, Figure 2a) reflects incipient ridgebuilding directly downstream of Katia in the simulation with ET (CTRL). Further downstream (50–35°W), the equatorward deflection of the midlatitude upper-level waveguide (blue 4 PVU contour) and positive difference PV (red shading, Figure 2a) reflect incipient downstream development in CTRL.

One day later, strong ridgebuilding occurs directly downstream of Katia (difference PV<-7 PVU, blue shading Figure 2b, cf. Figures 1c and 1d). The ridgebuilding is due to strong diabatic outflow by the transitioning TC, indicated by anticyclonically turning difference wind to the north of Katia (vectors in Figure 2b). The lowest
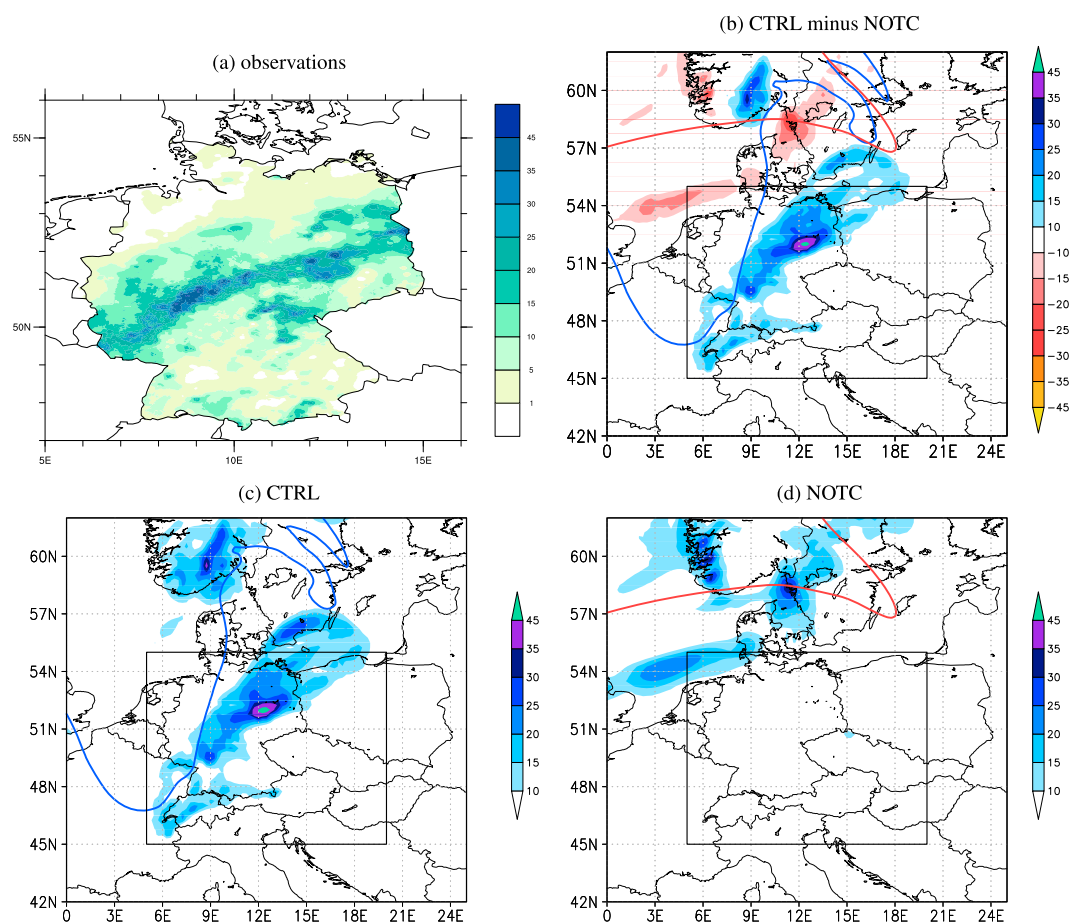
**Figure 3.** Accumulated precipitation in the 24 h period from 06 UTC, 11 September to 06 UTC, 12 September 2011 in (a) high-resolution gridded observations for Germany (kg m$^{-2}$; DWD REGNIE data), and in (b,c, and d) COSMO simulations (shaded kg m$^{-2}$) and PV on 335 K isentropic surface at 18 UTC, 11 September 2011 (blue/red 4 PVU contour for CTRL/NOTC). Figure 3b shows difference in precipitation in the CTRL simulation minus NOTC simulation, Figure 3c precipitation in the CTRL simulation, and Figure 3d precipitation in the NOTC simulation. Black box indicates the region used to compute the spatially averaged fields shown in Figure 4.

values of difference PV occur just south of the midlatitude waveguide in CTRL (blue 4 PVU contour), indicating that the poleward advection of diabatically produced low-PV air by the outflow of Katia enhances the tropopause PV gradient. Consequently, strongest westerly difference winds are centered around the midlatitude waveguide in CTRL (50°W to 30°W, 52°N; Figure 2b) in the region where the westward extension of the 50 m s$^{-1}$ is observed (cf. Figure 1c). The ridgebuilding triggers an important amplification of the downstream trough "T," which broadened and exhibits positive difference PV of >7 PVU (red shading Figure 2b, cf. Figure 1c). No flow amplification occurs in the NOTC simulation (red 4 PVU contour) and rather zonal flow persists. However, the short-wave trough amplified, propagated faster downstream, and is now located over the British Isles.

Until 18 UTC, 11 September 2011, the time of the HIW event in Central Europe, the ridge-trough couplet triggered by the ET of Katia further amplified and the upper-level midlatitude flow in the presence of ET (CTRL) is characterized by a pronounced Rossby wave pattern (Figure 2c, cf. Figures 1e and 1f). The ridge directly downstream of Katia now extends over a much larger region with difference PV widely below −7 PVU (blue shading, Figure 2c). The downstream trough dramatically elongates into a narrow PV streamer over Central Europe with its axis at 5°E. Difference PV reaches values of widely above 7 PVU in the PV streamer (red shading Figure 2c, cf. Figure 1e) and strong southerly difference wind establishes at its eastern flank (vectors in Figure 2c). In the absence of ET (NOTC), the upper-level flow remains zonally aligned but tilted to more west southwesterly flow from the subtropical Atlantic toward the British Isles and Scandinavia (red 4 PVU contour in Figure 2c). The short-wave trough propagated into the Baltic Sea. In the CTRL simulation with ET this short-wave trough

is also present. However, it rather results from diabatic outflow of the convection over eastern Germany and associated ridgebuilding at the eastern flank of the PV streamer (T) over Central Europe (cf. Figures 1e and 1f).

In summary, the comparison of the upper-level flow evolution in the sensitivity experiments with and without ET revealed that the interaction of Hurricane Katia with the midlatitude flow results in the formation of a pronounced upper-level ridge directly downstream of the transitioning TC. The ridgebuilding subsequently triggers downstream development that is manifested in a highly amplified PV streamer over Central Europe. In the absence of Katia, neither the eastern North Atlantic ridge nor the Central European PV streamer would be present and west southwesterly flow would prevail over the Atlantic-European region.

## 5. Katia's Role in Central European High-Impact Weather

Having shown that Katia actually triggers the downstream PV streamer, we explore the physical processes that link the PV streamer to the HIW observed in Central Europe.

High-resolution gridded observations for Germany in the 24 h period centered around the HIW event (Figure 3a; DWD REGNIE data [*Rauthe et al.*, 2013]) indicates that Central and Eastern Germany are predominantly affected by heavy precipitation. Maxima of more than 45 mm $(24 h)^{-1}$ occur in the Central German Uplands and in Eastern Germany (Figure 3a). A similar region is affected in the CTRL simulation, although maxima of more than 45 mm $(24 h)^{-1}$ occur in Eastern Germany only (Figures 3b and 3c). The difference in accumulated precipitation between the simulation with ET of Katia and the simulation without ET indicates that heavy precipitation in Central Europe only occurs in the presence of ET and ahead of the downstream PV streamer (Figures 3b and 3c). Precipitation is also enhanced in southern Norway in the presence of ET. In contrast, no significant precipitation occurs without ET over Central Europe (Figures 3b and 3d) but precipitation is slightly enhanced over Southwestern Norway, the North Sea, and Southwestern Sweden (Figures 3b and 3d). The shift of precipitation patterns over the North Sea and Scandinavia can be attributed to the more zonal west southwesterly flow from the Subtropics in the absence of ET (cf. PV contour in Figures 3b and 3d, discussion of Figure 2c, and discussion of Figures S2, S4, and Text S3).

In the following we explore the physical processes triggering the HIW event in Central Europe ahead of the PV streamer. Therefore, precipitation, mixed-layer convective available potential energy (CAPE), and quasi-geostrophic (QG) forcing from upper levels ($\leq 650$ hPa) for ascending motion at 700 hPa are spatially averaged in a rectangular box over the region affected by HIW (5–20°E, 45–55°N; black rectangle in Figures 3, S3, and S4). The temporal evolution of these spatially averaged quantities is then evaluated for the CTRL and NOTC simulations (Figure 4). A temporal sequence of spatial maps is discussed in Text S3.

Until about 18 UTC, 10 September 2011, the temporal evolution of precipitation, CAPE and QG forcing for ascending motion over Central Europe is similar in CTRL and NOTC, because there is no downstream impact of ET in the target region, yet (Figure 4, cf. Figures S2a–S2d). As a side remark, we note that this also confirms a good representation of the environmental background flow in the simulation without ET (NOTC) with respect to CTRL. Important differences evolve with the approaching PV streamer in CTRL on 11 September. Due to the ongoing advection of warm, moist air from the South (see Text S3, Figures S2e, S2f, and S4,) box-averaged CAPE increases dramatically during 11 September 2011 in the presence of ET, with a maximum of 290 J $kg^{-1}$ at 16 UTC, 11 September 2011 (red in Figure 4a). With a few hours delay, upper-level QG forcing for ascending motion, induced by the approaching PV streamer increases and peaks at 0.0048 m $s^{-1}$ at 18 UTC, 11 September 2011 (green in Figure 4a). This forcing triggers a sudden release of CAPE as vigorous thunderstorms evolve and results in a peak of box-averaged 6 h accumulated precipitation (2.97 mm from 18 UTC, 11 to 00 UTC, 12 September 2011; blue in Figure 4a). In the absence of the PV streamer (NOTC, Figure 4b) the air mass over Central Europe does not exhibit high values of CAPE, and only weak forcing for ascending motion exists in the afternoon of 11 September 2011. Thus, the key ingredients for the HIW event are missing and no heavy precipitation event occurs. However, higher values of QG forcing and slightly enhanced precipitation occur along with the passage of the short-wave trough "t" earlier (0.42 mm from 00 UTC to 06 UTC, 11 September 2011 in NOTC versus 0.19 mm in CTRL).

In summary, the PV streamer, which is triggered as a downstream response to ridgebuilding by the ET of Katia, is key to the Central European HIW several thousands of kilometers downstream of the transitioning TC. The PV streamer leads to the advection of warm, moist air to Central Europe. During 11 September 2011 high values of CAPE build up in this air mass. Along with strong upper-level forcing for ascending motion, directly related
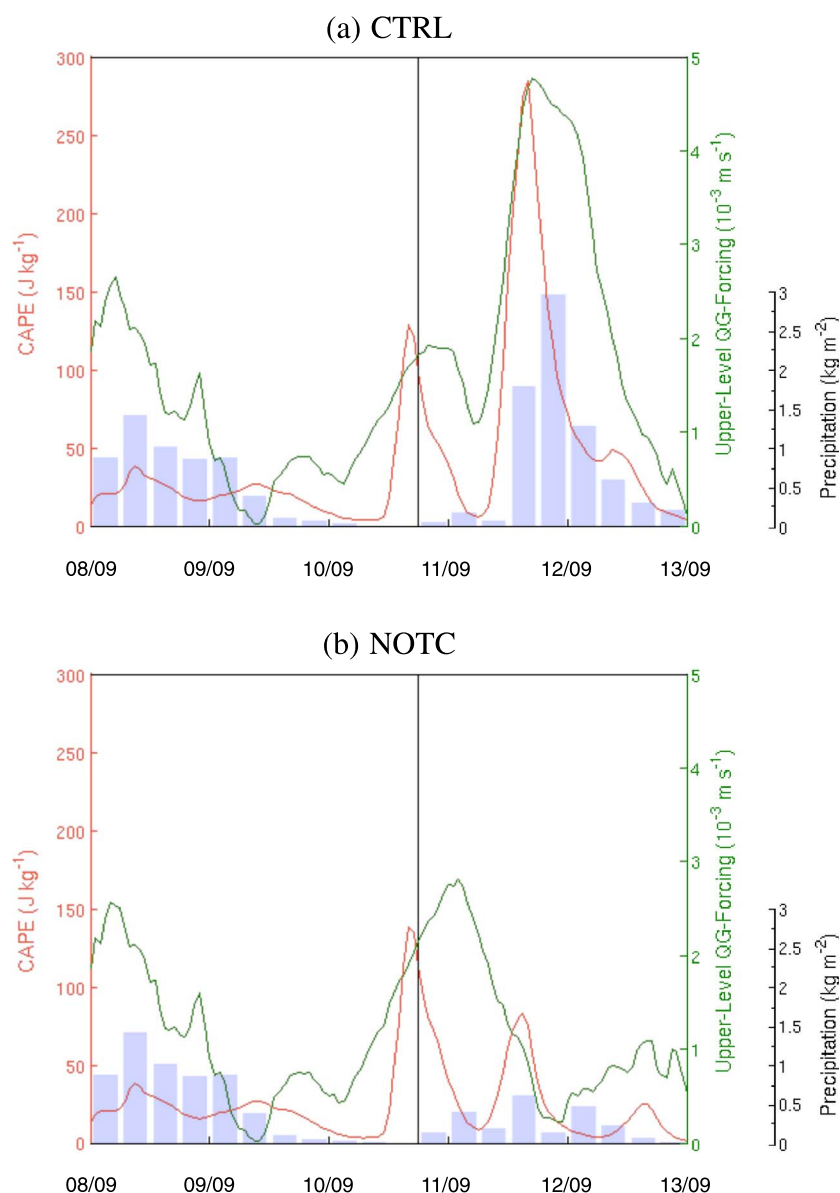
**Figure 4.** Spatial average (5°E–20°E, 45°N–55°N) of precipitation (blue columns in kg m$^{-2}$, $y$ axis (black) on the right), mixed-layer CAPE (red in J kg$^{-1}$, $y$ axis on the left) and QG forcing from upper levels ($\leq$650 hPa) for ascending motion at 700 hPa (green in 10$^{-3}$m s$^{-1}$, $y$ axis on the right). (a) CTRL simulation and (b) NOTC simulation. $X$ axis labeled with date/month 2011 at 00 UTC. Hourly data shown for CAPE and QG forcing, 6-hourly accumulated precipitation for period spanned by respective column. A vertical line at 18 UTC, 10 September is shown.

to the PV streamer, this CAPE is released, resulting in strong convection and associated heavy precipitation in Eastern Germany. This key mechanism is completely missing in the absence of ET. The proposed mechanism is also evident in ECMWF analyses (Text S4 and Figures S5 and S6).

One may argue that HIW still existed without ET but at a different location or time. Indeed, neither an earlier nor a later precipitation event occurs over Central Europe in NOTC (Figure 4b). However, the NOTC simulation indicates a region of precipitation stretching from the British Isles to Southern Scandinavia, along with the more zonal flow in the absence of ET (Figures 3b and 3d). Hence, the ET of Katia causes HIW in Central Europe far downstream of the transforming TC, and by modifying the large-scale flow, it likewise alters the region affected by HIW farther to the north.

## 6. Conclusion

This study investigates the impact of Hurricane Katia on the midlatitude flow over the North Atlantic-European region in September 2011. Using a TC removal technique [*Grams et al.*, 2013b] we show that the ET of Katia is key to important upper-level midlatitude flow modifications which subsequently cause high-impact weather in Central Europe far downstream of the actual TC undergoing ET. Our key findings are as follows:

1. The interaction of North Atlantic Hurricane Katia (2011) with the midlatitude flow *caused* strong upper-level ridgebuilding and a subsequent downstream trough that amplified into a narrow PV streamer over Central Europe.
2. In the absence of ET zonal west southwesterly flow would prevail over the Atlantic-European region.
3. Ahead of the PV streamer warm and moist air was advected into Central Europe, and high values of CAPE built up during 11 September 2011. Upper-level QG forcing by the approaching PV streamer released the CAPE, resulting in vigorous deep convection.
4. Without ET, the PV streamer and associated HIW were not present. Thus, Central European HIW was caused by Katia as an important downstream impact of North Atlantic ET.

Research on ET is motivated by its impact on the midlatitude flow and high-impact weather in regions far downstream of ET. Important differences for the strength of the downstream impact of ET have been found for different ocean basins [e.g., *Quinting and Jones*, 2015; *Torn and Hakim*, 2015]. In these studies downstream impact of ET in the North Atlantic is weaker compared to other ocean basins. Likewise, *Pantillon et al.* [2015] concluded that the downstream impact of North Atlantic ET is rather a perturbation to midlatitude wave breaking than a cause.

To the best of our knowledge the results presented here, first, clearly document that strong upper-level midlatitude flow modification and associated European high-impact weather can be caused by the *downstream impact* of a transitioning North Atlantic TC. Therefore, our study confirms a basic motivation for ET research and corroborates the need for an in-depth process understanding of ET in order to improve numerical weather forecasts in the midlatitudes during ET episodes. The TC removal technique employed here, allows a clear attribution of flow modification to the presence of ET, but is intrinsically bound to case studies. A more climatological study would be needed to investigate how frequent ET triggers downstream HIW and whether a systematic linkage exists. Due to the need for numerical experiments for each case, such a climatological study is extensive. Work is currently in progress on a hybrid approach combining the case-study and composite approaches.

## References

Agustí-Panareda, A., C. Thorncroft, G. Craig, and S. Gray (2004), The extratropical transition of hurricane Irene (1999): A potential-vorticity perspective, *Q. J. R. Meteorol. Soc.*, *130*(598), 1047–1074, doi:10.1256/qj.02.140.

Agustí-Panareda, A., S. L. Gray, G. C. Craig, and C. Thorncroft (2005), The extratropical transition of tropical cyclone Lili (1996) and its crucial contribution to a moderate extratropical development, *Mon. Weather Rev.*, *133*(6), 1562–1573.

Aiyyer, A. (2015), Recurving western North Pacific tropical cyclones and midlatitude predictability, *Geophys. Res. Lett.*, *42*, doi:10.1002/2015GL065082.

Anwender, D., P. A. Harr, and S. C. Jones (2008), Predictability associated with the downstream impacts of the extratropical transition of tropical cyclones: Case studies, *Mon. Weather Rev.*, *136*(9), 3226–3247, doi:10.1175/2008MWR2249.1.

Archambault, H. M. (2007), Recurving typhoons as precursors to an early season Arctic outbreak over the continental U.S., *paper presented at Ninth Northeast Regional Operational Workshop*, National Weather Service/Am. Meteor. Soc., Albany, New York. [Available at http://cstar.cestm.albany.edu/nrow/nrow9/Archambault/archambault.ppt.]

Archambault, H. M. (2011), The downstream extratropical flow response to recurving western North Pacific tropical cyclones, PhD thesis, Univ. of Albany, New York.

Archambault, H. M., L. F. Bosart, D. Keyser, and J. M. Cordeira (2013), A climatological analysis of the extratropical flow response to recurving Western North Pacific tropical cyclones, *Mon. Weather Rev.*, *141*(7), 2325–2346, doi:10.1175/MWR-D-12-00257.1.

Archambault, H. M., D. Keyser, L. F. Bosart, C. A. Davis, and J. M. Cordeira (2015), A composite perspective of the extratropical flow response to recurving Western North Pacific tropical cyclones, *Mon. Weather Rev.*, *143*, 1122–1141, doi:10.1175/MWR-D-14-00270.1.

Atallah, E. H., and L. F. Bosart (2003), The extratropical transition and precipitation distribution of Hurricane Floyd (1999), *Mon. Weather Rev.*, *131*(6), 1063–1081.

Blumer, S. R. (2013), The downstream impact of extratropical transition during the North Atlantic Hurricane Season 2011, Master's thesis, Inst. for Atmos. and Clim. Sci., ETH Zurich, Switzerland.

Bosart, L. F., and G. M. Lackmann (1995), Postlandfall tropical cyclone reintensification in a weakly baroclinic environment: A case study of Hurricane David (September 1979), *Mon. Weather Rev.*, *123*(11), 3268–3291, doi:10.1175/1520-0493(1995)123<3268:PTCRIA>2.0.CO;2.

Böttcher, M., and H. Wernli (2011), Life cycle study of a diabatic Rossby wave as a precursor to rapid cyclogenesis in the North Atlantic—Dynamics and forecast performance, *Mon. Weather Rev.*, *139*(6), 1861–1878, doi:10.1175/2011MWR3504.1.

Browning, K. A., P. Panagi, and G. Vaughan (1998), Analysis of an ex-tropical cyclone after its reintensification as a warm-core extratropical cyclone, *Q. J. R. Meteorol. Soc.*, *124*(551), 2329–2356.

Clough, S. A., C. S. A. Davitt, and A. J. Thorpe (1996), Attribution concepts applied to the omega equation, *Q. J. R. Meteorol. Soc.*, *122*(536), 1943–1962, doi:10.1002/qj.49712253610.

Cordeira, J. M., and L. F. Bosart (2010), The antecedent large-scale conditions of the "Perfect Storms" of late October and early November 1991, *Mon. Weather Rev.*, *138*, 2546–2569, doi:10.1175/2010MWR3280.1.

Dacre, H. F., and S. L. Gray (2009), The spatial distribution and evolution characteristics of North Atlantic cyclones, *Mon. Weather Rev.*, *137*(1), 99–115, doi:10.1175/2008MWR2491.1.

Deveson, A. C. L., K. A. Browning, and T. D. Hewson (2002), A classification of FASTEX cyclones using a height-attributable quasi-geostrophic vertical-motion diagnostic, *Q. J. R. Meteorol. Soc.*, *128*(579), 93–117, doi:10.1256/00359000260498806.

DiMego, G. J., and L. F. Bosart (1982), The transformation of tropical storm Agnes into an extratropical cyclone. Part I: The observed fields and vertical motion computations, *Mon. Weather Rev.*, *110*(5), 385–411, doi:10.1175/1520-0493(1982)110<0385:TTOTSA>2.0.CO;2.

Ehmann, C., and B. Mühr (2011), Heftige Gewitter, Mitteleuropa, 11.09.2011 [in German], Tech. Rep., Wettergefahren-Frühwarnung, IMK-TRO/CEDIM, KIT, Karlsruhe, Germany. [Available at http://www.wettergefahren-fruehwarnung.de/Ereignis/20110913_e.html retrieved at 15 July 2015.]

Evans, J. L., and R. E. Hart (2003), Objective indicators of the life cycle evolution of extratropical transition for Atlantic tropical cyclones, *Mon. Weather Rev.*, *131*(5), 909–925, doi:10.1175/1520-0493(2003)131<0909:OIOTLC>2.0.CO;2.

Grams, C. M. (2011), Quantification of the downstream impact of extratropical transition for Typhoon Jangmi and other case studies, PhD thesis, Karlsruhe Inst. of Technol., Karlsruhe, Germany.

Grams, C. M., H. Wernli, M. Böttcher, J. Čampa, U. Corsmeier, S. C. Jones, J. H. Keller, C.-J. Lenz, and L. Wiegand (2011), The key role of diabatic processes in modifying the upper-tropospheric wave guide: A North Atlantic case-study, *Q. J. R. Meteorol. Soc.*, *137*(661), 2174–2193, doi:10.1002/qj.891.

Grams, C. M., S. C. Jones, and C. A. Davis (2013a), The impact of Typhoon Jangmi (2008) on the midlatitude flow. Part II: Downstream evolution, *Q. J. R. Meteorol. Soc.*, *139*(677), 2165–2180, doi:10.1002/qj.2119.

Grams, C. M., S. C. Jones, C. A. Davis, P. A. Harr, and M. Weissmann (2013b), The impact of Typhoon Jangmi (2008) on the midlatitude flow. Part I: Upper-level ridgebuilding and modification of the jet, *Q. J. R. Meteorol. Soc.*, *139*(677), 2148–2164, doi:10.1002/qj.2091.

Grams, C. M., J. H. Keller, and S. T. K. Lang (2015), A quantitative assessment of the sensitivity of the downstream midlatitude flow response to extratropical transition of tropical cyclones, *Geophys. Res. Lett.*, doi:10.1002/2015GL065764.

Harr, P. A., and J. M. Dea (2009), Downstream development associated with the extratropical transition of tropical cyclones over the Western North Pacific, *Mon. Weather Rev.*, *137*(4), 1295–1319, doi:10.1175/2008MWR2558.1.

Hart, R. E., and J. L. Evans (2001), A climatology of the extratropical transition of Atlantic tropical cyclones, *J. Clim.*, *14*(4), 546–564.

Hoskins, B., and P. Berrisford (1988), A potential vorticity perspective of the storm of 15–16 October 1987, *Weather*, *43*(3), 122–129, doi:10.1002/j.1477-8696.1988.tb03890.x.

Hoskins, B. J., I. Draghici, and H. C. Davies (1978), A new look at the $\omega$-equation, *Q. J. R. Meteorol. Soc.*, *104*(439), 31–38, doi:10.1002/qj.49710443903.

Jones, S. C., et al. (2003), The extratropical transition of tropical cyclones: Forecast challenges, current understanding, and future directions, *Weather Forecasting*, *18*(6), 1052–1092.

Keller, J. H., and C. M. Grams (2014), Investigating the impact of Typhoon Choi-Wan (2009) on the mid-latitude flow using eddy kinetic energy analysis, *paper presented at 31st Conf. on Hurricanes and Tropical Meteorology*, pp. 170, Am. Meteorol. Soc, San Diego, Calif.

Keller, J. H., S. C. Jones, J. L. Evans, and P. A. Harr (2011), Characteristics of the TIGGE multimodel ensemble prediction system in representing forecast variability associated with extratropical transition, *Geophys. Res. Lett.*, *38*, L12802, doi:10.1029/2011GL047275.

Keller, J. H., S. C. Jones, and P. A. Harr (2014), An eddy kinetic energy view of physical and dynamical processes in distinct forecast scenarios for the extratropical transition of two tropical cyclones, *Mon. Weather Rev.*, *142*(8), 2751–2771, doi:10.1175/MWR-D-13-00219.1.

Klein, P. M., P. A. Harr, and R. L. Elsberry (2000), Extratropical transition of western North Pacific tropical cyclones: An overview and conceptual model of the transformation stage, *Weather Forecasting*, *15*(4), 373–395.

Klein, P. M., P. A. Harr, and R. L. Elsberry (2002), Extratropical transition of Western North Pacific tropical cyclones: Midlatitude and tropical cyclone contributions to reintensification, *Mon. Weather Rev.*, *130*(9), 2240–2259, doi:10.1175/1520-0493(2002)130<2240:ETOWNP>2.0.CO;2.

Knapp, K. R., et al. (2011), Globally gridded satellite observations for climate studies, *Bull. Am. Meteorol. Soc.*, *92*(7), 893–907, doi:10.1175/2011BAMS3039.1.

McTaggart-Cowan, R., J. R. Gyakum, and M. K. Yau (2001), Sensitivity testing of extratropical transitions using potential vorticity inversions to modify initial conditions: Hurricane Earl case study, *Mon. Weather Rev.*, *129*(7), 1617–1636, doi:10.1175/1520-0493(2001)129<1617:STOETU>2.0.CO;2.

McTaggart-Cowan, R., J. R. Gyakum, and M. K. Yau (2004), The impact of tropical remnants on extratropical cyclogenesis: Case study of Hurricanes Danielle and Earl (1998), *Mon. Weather Rev.*, *132*(8), 1933–1951, doi:10.1175/1520-0493(2004)132<1933:TIOTRO>2.0.CO;2.

Pantillon, F., J.-P. Chaboureau, and E. Richard (2015), Remote impact of North Atlantic hurricanes on the Mediterranean during episodes of intense rainfall in autumn 2012, *Q. J. R. Meteorol. Soc.*, *141*(688), 967–978, doi:10.1002/qj.2419.

Quinting, J. F., and S. C. Jones (2015), On the impact of tropical cyclones on Rossby wave packets: A climatological perspective, *Mon. Weather Rev.*, doi:10.1175/MWR-D-14-00298.1.

Rauthe, M., H. Steiner, U. Riediger, A. Mazurkiewicz, and A. Gratzki (2013), A Central European precipitation climatology Part I: Generation and validation of a high-resolution gridded daily data set (HYRAS), *Meteorol. Z.*, *22*(3), 235–256, doi:10.1127/0941-2948/2013/0436.

Riemer, M., and S. C. Jones (2010), The downstream impact of tropical cyclones on a developing baroclinic wave in idealized scenarios of extratropical transition, *Q. J. R. Meteorol. Soc.*, *136*(648), 617–637, doi:10.1002/qj.605.

Riemer, M., S. C. Jones, and C. A. Davis (2008), The impact of extratropical transition on the downstream flow: An idealized modelling study with a straight jet, *Q. J. R. Meteorol. Soc.*, *134*(630), 69–91, doi:10.1002/qj.189.

Ritchie, E. A., and R. L. Elsberry (2007), Simulations of the extratropical transition of tropical cyclones: Phasing between the upper-Level trough and tropical cyclones, *Mon. Weather Rev.*, *135*(3), 862–876, doi:10.1175/MWR3303.1.

Steppeler, J., G. Doms, U. Schättler, H. W. Bitzer, A. Gassmann, U. Damrath, and G. Gregoric (2003), Meso-gamma scale forecasts using the nonhydrostatic model LM, *Meteorol. Atmos. Phys.*, *82*, 75–96, doi:10.1007/s00703-001-0592-9.

Stewart, S. R. (2012), Tropical Cyclone Report: Hurricane Katia (AL122011) 29 August–10 September 2011, Tech. Rep., National Hurricane Center, http://www.nhc.noaa.gov/data/tcr/index.php?season=2011&basin=atl retrieved at 15 July 2015, Miami, Fla.

Stohl, A., C. Forster, and H. Sodemann (2008), Remote sources of water vapor forming precipitation on the Norwegian west coast at 60°N—A tale of hurricanes and an atmospheric river, *J. Geophys. Res.*, *113*, D05102, doi:10.1029/2007JD009006.

Thorncroft, C., and S. C. Jones (2000), The extratropical transitions of Hurricanes Felix and Iris in 1995, *Mon. Weather Rev.*, *128*(4), 947–972, doi:10.1175/1520-0493(2000)128<0947:TETOHF>2.0.CO;2.

Thorncroft, C. D., B. J. Hoskins, and M. E. McIntyre (1993), Two paradigms of baroclinic-wave life-cycle behaviour, *Q. J. R. Meteorol. Soc.*, *119*(509), 17–55, doi:10.1002/qj.49711950903.

Torn, R. D., and G. J. Hakim (2015), Comparison of wave packets associated with extratropical transition and winter cyclones, *Mon. Weather Rev.*, *143*(5), 1782–1803, doi:10.1175/MWR-D-14-00006.1.

Wu, C.-C., and Y. Kurihara (1996), A numerical study of the feedback mechanisms of Hurricane-environment interaction on Hurricane movement from the potential vorticity perspective, *J. Atmos. Sci.*, *53*(15), 2264–2282, doi:10.1175/1520-0469(1996)053<2264:ANSOTF>2.0.CO;2.

### Erratum

In the originally published version of this article, the Supporting Information contained formatting errors. The file format error have since been corrected, and this version may be considered the authoritative version of record.